Arabian Journal of Chemistry (2020) 13, 4553–4563

King Saud University

Arabian Journal of Chemistry

www.ksu.edu.sa
www.sciencedirect.com

ORIGINAL ARTICLE

Graphene oxide decorated bimetal (MnNi) oxide nanoflakes used as an electrocatalyst for enhanced oxygen evolution reaction in alkaline media

Siva Prasad Mooni [a,1], Kiran Kumar Kondamareddy [c], Sunling Li [a], Xin Zhou [a], Liu Chang [a], Xia Ke [a], Xiaoqiang Yang [a], Dan Li [b], Qing Qu [a,1,*]

[a] *School of Chemical Science and Technology, Yunnan University, Kunming 650091, China*
[b] *The State Key Laboratory for Refractories and Metallurgy, School of Materials and Metallurgy, Wuhan University of Science and Technology, Wuhan 430081, China*
[c] *Department of Physics, School of Pure Sciences, College of Engineering Science and Technology, FIJI National University, Natabua Campus, Lautoka 5529, Fiji*

Received 2 August 2019; accepted 8 October 2019
Available online 16 October 2019

KEYWORDS

MnO_2;
NiO;
Graphene oxide;
Electrodeposition;
Alkaline solution;
Annealing;
OER

Abstract Precious non-noble metals have been constantly attracting research attention in order to realize an inexpensive, extra active and more stable electrocatalysts in terms of various oxidation states and structures for their applications in oxidation (splitting) of water. In the present work graphene oxide incorporated, MnO_2-NiO composite metal oxide nanoflakes were synthesized on the stainless steel substrate using efficient electrodeposition route in alkaline media and drop casting method with further annealing treatment at 400 °C for 4 h. Initially MnO_2-NiO nanoflakes were deposited using different cyclic sweep rates, later graphene oxide suspension was drop casted on the MnO_2-NiO nanoflakes and subsequently subjected to annealing at 200 °C for 2 h. The prepared electrode material is denoted as GO/MnO_2-NiO/SS and used as an electrocatalyst for oxygen evolution. Field emission scanning electron microscopy, transmission electron microscopy, Energy dispersive electron spectroscopy and X-ray diffraction spectroscopy were used to study the crystalline nature and morphologies of the deposited films. The electrochemical properties of the electrode material were investigated using cyclic voltammetry and linear sweep voltammetry. The electrode exhibits low overpotential and small Tafel slope of 379 mV and 47.84 $mVdec^{-1}$ at the current density of 10 mA cm^{-2} in alkaline (KOH) medium. In addition, the electrode shows a long time stability of 28800 s. Hence, the present study suggests that the GO incorporated Mn-Ni bimetal oxide

* Corresponding author.
E-mail addresses: sivaphdchem@gmail.com (S.P. Mooni), quqing@yun.edu.cn (Q. Qu).
[1] Future Communication

Peer review under responsibility of King Saud University.

Production and hosting by Elsevier

https://doi.org/10.1016/j.arabjc.2019.10.003

modified electrode is suitable electrode material for oxygen evolution reaction (OER), owing to its facile preparation, inexpensive, easy handling and high active nature.

1. Introduction

Global environmental problems and demand for clean energy became severe concern in recent years. The exploration, preparation and synthesis of novel energy materials with various nanostructures for high surface area have become the focus of recent research. The potentiality, clean production methods and elevated performance make hydrogen as a promising alternate candidate for the fossil fuels (Xie et al., 2103, Darabdhara et al., 2015). Hydrogen can be simply obtained from water putrefaction by using renewable energy sources such as wind and solar energies (Chu and Majumdar, 2012; Guio Morales et al., 2014). In spite of this, electrolysis of water is an enormously competent way to generate hydrogen (Chu and Majumdar, 2012; Guio Morales et al., 2014; Yan et al. 2018; Tan et al., 2017). The water catalysis involves two reactions, one is the hydrogen evolution reaction (HER) and other is the oxygen evolution reaction (OER) (Yang et al., 2017; Chi et al 2017; Wang et al., 2018; park et al., 2012]. During the catalytic reaction the catalyst can significantly reduce the energy barrier in these two reactions. Pt-based and Ir/Ru-based materials are potential mediating catalysts for water splitting. Despite of high catalytic activity of these noble metal-based catalysts, their highs cost, scarcity and poor stability limit their applications (Zou and Zhang, 2015; Lee et al., 2012; Reier et al., 2012; Antolini, 2014; Danilovic et al., 2014; Oh et al., 2015; Browne et al., 2016). In order to realize more practical and competent catalysts for extensive applications, the catalysts must be based on common materials and the methods of preparation of catalysts must be as simple as achievable. Precious non-noble metals have been continuously attracting research attention in order to understand an inexpensive, extra active and more stable electrocatalysts for their applications in oxidation (splitting) of water. Many researchers have synthesized various catalysts, based on the transition metal-based compounds including metals and metal oxides (McKone et al., 2013; Zhang et al., 2016a; Zhang et al., 2016b; Zhenhua et al., 2018; Arpita et al., 2017; Michael et al., 2015; Zhang et al., 2016c) for effectual water splitting (HER and OER).

The oxygen evolution reaction (OER) plays a significant role in evolving clean energy and storage technologies, as it produces electrons that can split the water in to hydrogen, carbon dioxide in to carbon containing fuels, and metal ions in to metals during recharge of metal–air batteries (Suntivich et al., 2011; Oh et al., 2012; Wang, 2015; Lu and Zhao, 2015). The devices associated with OER for various industrial and other applications mostly rely on low-cost, abundant and promising electrocatalysts that support slow processes involving transfer of four electrons (Morales Guio et al., 2016). Increasing the loaded mass is one of the feasible ways to attain high current at reasonable overpotential, but this method can hinder mass and charge transfer (Batchellor, 2015). Further, an additional impenetrability of catalysts observed at high OER currents results in to an exhaustive bubble release, which in turn causes unfavorable bubble-shielding effect and catalyst detachment problem (Lu and Zhao, 2015). Thus efficient electrocatalysts are required, in order to accelerate the reaction, limit the overpotential and thus improve the energy conversion competence. Various catalysts, based on the combination of metal, metal oxides/hydroxides and graphene composites, such as cobalt oxide, titanium oxide, nickel oxide, manganese oxide, Ni–Fe oxide, Ni-Mn oxide, Ni-Co oxide, Zn–Co and so on oxide based materials have been extensively developed for OER (Singh et al., 2015; Li et al., 2019; Yan et al., 2019; Wang et al., 2019; Hutchings et al., 2015; Huang et al., 2019; Yushuai et al., 2017; Wu et al., 2016; Menezes et al., 2015; Song and Hu, 2014; Rong et al., 2015; Qiao et al., 2015; Zhuang et al., 2015; Can et al., 2018; Senthil et al., 2018; Wu et al., 2019; Pei et al. 2019). Manganese is one among those metals which is an abundant element and manganese oxides (MnO_2) have been previously investigated to achieve high activity for the oxygen evolution reaction (Takashima et al., 2012; Kang et al., 2017; Chen ett al., 2014; Li et al., 2015; Prasad et al., 2020). Although graphene based materials are also superior electrocatalyst (Wan et al., 2015), the better performance of MnO_2-NiO remains unchallenged by any pure graphene materials. Yang et al. (2012) used MnO_2-graphene nanosheets as the air cathode in lithium-air cells and obtained a discharge capacity much higher than pure graphene nanosheets (GNS) catalyst. For further improvement of the properties OER, significant efforts have to be put forward by preparing metal oxides and graphene based composite materials.

However few reports were found in the literature, on the combination of manganese, nickel oxide and graphene oxide composite materials previously. Hwang et al. (2013) reported on preparation of graphene-NiO-MnO_2 nanocomposite. The catalyst was formed by a simple chemical precipitation method using a chelating agent and Ni and Mn hydroxides on graphene for supercapacitors applications (Wan et al., 2015). Rusi et al. (2016) investigated on the effects of electrodeposition mode and deposition cycle of NiO-MnO_2 composite electrodes on the electrochemical performance for high energy density supercapacitors. Lee et al. (2014) prepared manganese-nickel oxide films on a graphite sheet using electro-deposition technique for electrochemical capacitor applications. Tran et al. (2015) synthesized nanoflake manganese oxide and nickel-manganese oxide using electrodeposition for electrochemical capacitors applications. Ye et al. (2017) reported on various metal ions doped-MnO_2 ultrathin nanosheets for catalysis applications. All the above methods either involve a separate synthesis of each material, followed by combining of all the materials once or layer by layer synthesis in multistep process by electro-deposition method. However it is found that there is a difficulty in achieving homogeneous nanostructures over the substrates. In case of our method the electrodeposition of bimetal hydroxides deposited at a single

step in alkaline media with homogenous nanostructure and it is significant, very simple, selective and sensitive compared to the literature methods reported in the literature.

In the present work we developed a facile method for preparing the electrode using a composite of bimetallic oxides (Mn-Ni) and graphene oxide by employing combined simple electrodeposition and drop casting methods in alkaline solution. Subsequent annealing for a short period led to form a homogenous nanostructure. In this method deposition cycles, annealing time and annealing temperatures play a significant role in the formation of homogeneous nanostructure. To the best of our knowledge we didn't find any report on the method which employs the combination of the materials particularly for oxygen evolution reaction.

2. Experimental

2.1. Materials and reagents

The stainless steel foil with 99% purity (with measurements 15 × 35 × 1 mm) was purchased from Good fellow, China. All chemicals, manganese acetate tetra hydrate ($Mn(CH_3COO)_2{\cdot}4H_2O$), nickel acetate tetra hydrate ($Ni(CH_3COO)_2{\cdot}4H_2O$), sodium sulphate ($Na_2SO_4$), sodium hydroxide (NaOH), sulfuric acid (H_2SO_4) and graphene oxide (GO) which are standard analytically reagent graded, were purchased from Sino pharmchemical reagent company and used as usual without additional purification. Deionized water (DI) was used in all aqueous solutions.

2.2. Instrumentation for characterization

All electrochemical experiments such as cyclic voltammetry, linear sweep voltammetry, amperometry and electrochemical impedance spectroscopy (EIS) were carried out using a CHI 660E (CH Instrument Company of Shanghai, China) electrochemical work station (potentiostat/galvanostat). A three electrode system which contains GO/MnO_2-NiO modified electrode, Pt wire and Ag/AgCl, SCE as working electrode; counter electrode and reference electrode respectively is used in 0.1 M KOH solution. For EIS, the applied frequencies are from 0.1 Hz to 10 kHz. X-ray diffraction studies were carried out (model XRD, Bruker AXS, Germany) using the Cu Kα radiation (λ = 1.5418 Å) and field-emission scanning electron microscopy (FE-SEM, FEI Nov. 450 Nano, USA) were used to study the morphology and nanostructure of the prepared electrodes. Further Transmission electron microscopy (TEM), (JEM-2100UHR STEM/EDS, JEOL, Japan) was used for characterization of the electrodes.

2.3. Preparation of graphene oxide incorporated MnO_2-NiO nanoflakes

The stainless steel sheet (35 × 15 × 1 mm) of model 316 L with 99% purity was used as substrate. Initially the stain steel substrate was mechanically polished using emery paper of different grades 500, 1000 and 1500, and an aluminium slurry as well, for attaining the mirror like surface. Subsequently the as polished substrate was cleaned ultrasonically in deionized water and ethanol for 10 min, and then dried in the stream of pure N_2. The deposition of electrolyte involve preparation of the mixture of 0.02 M Manganese (II) Acetate tetrahydrate ($Mn(CH_3COO)_2{\cdot}4H_2O$), 0.05 M Nickel acetate tetrahydrate ($Ni(CH_3COO)_2{\cdot}4H_2O$), and 0.5 M sulphuric acid (H_2SO_4) or 1.0 M Na_2SO_4 in a 250 mL beaker which is stirred magnetically for 30 min, and then obtained a homogeneous solution. Further, adequate electrolyte solution was transferred in to the electrochemical cell containing a three electrode system that employs electrodeposition method (cyclic sweep). The applied potentials at different scan rates (5–50 mV/s) are in the range of 0–1.4 V. A set of different cycles (6, 10, 20 cycles) for various alkaline and acidic solutions [for acidic solution see supplementary information (SI)], such as Na_2SO_4 and H_2SO_4 are employed. The obtained nano composite were annealed at various temperature and time intervals from 300 to 400 °C for 1.0 h to 6.0 h and finally got the uniformed nanoflakes. Here the formation of flakes occurred may be the oxidation state of Mn increases. Since it is improbable that two electrons are transferred in a single step, the formation of MnO_2 from Mn^{2+} occurs concomitantly with the oxidation of water molecules. Similarly nickel oxide makes simultaneously with MnO_2 use of nickel hydroxide precipitation. Nickel hydroxide is formed on the electrode, finally, the electrodeposition of nickel/manganese oxides in an electrolyte containing Mn^{2+}/Ni^{2+} ions (Lee et al., 2014). Based on the cyclic voltammetric response, the applied cyclic voltammetric cycles of 10 CV cycles at scan rate 20 mV/s (20/10) in alkaline solution were selected as optimum conditions and the obtained electrode was used for further analysis. Under these conditions well defined MnO_2-NiO nano flakes were obtained. Finally different amount of graphene oxide (10–50 μL) was drop casted on the as prepared MnO_2-NiO nano flakes, dried in air 5–6 h, then annealed at 200 °C for 2 h. During the annealing process the graphene oxide formed into a homogeneous layer on MnO_2-NiO nano flakes and the nano composite loaded on the substrate around 0.1 mg. The final obtained electrode

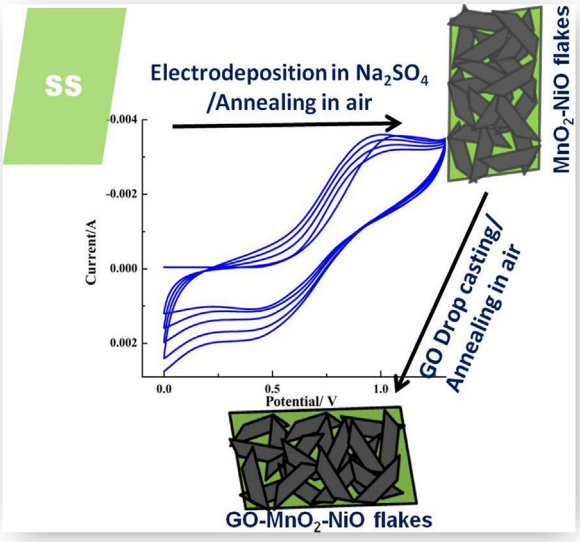

Scheme 1 The schematic representation of the electrode preparation at optimum conditions.

denoted as GO/MnO_2-NiO (10 GO, 20 GO, 30 GO and 50 GO), and used for further analysis. The schematic illustration of electrode preparation was depicted in Scheme 1.

3. Results and discussions

3.1. The electrochemical performance of the electrode

The bimetal oxide based nanostructure was deposited on the steel substrate by electro-deposition method (cyclic sweep). The bimetal hydroxide (OH) based nanostructure was formed on steel substrates by cyclic voltammetric sweeping between 0 V and 1.4 V at various scan rates 20 mV s^{-1}, 50 mV s^{-1} for different cycle segments after that annealed at 400°C for 4 h. Fig. 1, shows the cyclic voltamogrammes obtained at 50 mV s^{-1} for 6 segments (50/6) (A), 50 mV s^{-1} 10 segments (50/10) (B), 20 mV s^{-1} for 20 segments (20/20) (C), 20 mV s^{-1} for 10 segments (20/10) (D). The graphene oxide was drop casted on the as prepared MnO_2-NiO nanoflakes and subsequently annealed at 200°C for 2 h and GO layer was formed and exhibited various colours. The photographs of the as prepared electrodes are shown in Fig. S2. The prepared nanoflakes exhibited an improved electrochemical activity and surface area. The well-defined peeks were obtained at 20 mV s^{-1} for 10 (20/10) segments [Fig. 1D], and hence was selected as optimised sample and used for further analysis. The expected mechanism of electrode reaction based on bimetal oxide employs cyclic sweep mode can be described as follows (Scheme 2). Initially during the deposition process when the potential is applied water, molecule reduced at working electrode and produced hydroxyl ions. The as produced OH^- ions play a significant role in the growth of metal oxides over the steel substrate. It may be the instantaneous nucleation process. Then, a progressive nucleation process takes place, in which the flake structure grows. As the number of deposition segments (cycles) increases, the growth rate of the progressive nucleation also increases, resulting the nano flakes when main-

$$2H_2O + 2e^- \rightarrow H_2 + 2OH^-$$
$$Mn^{2+} + OH^- \rightarrow MnOOH \rightarrow MnO_2$$
$$Ni^{2+} + OH^- \rightarrow NiOH \quad \rightarrow NiO/\ GO\ added$$

Scheme 2

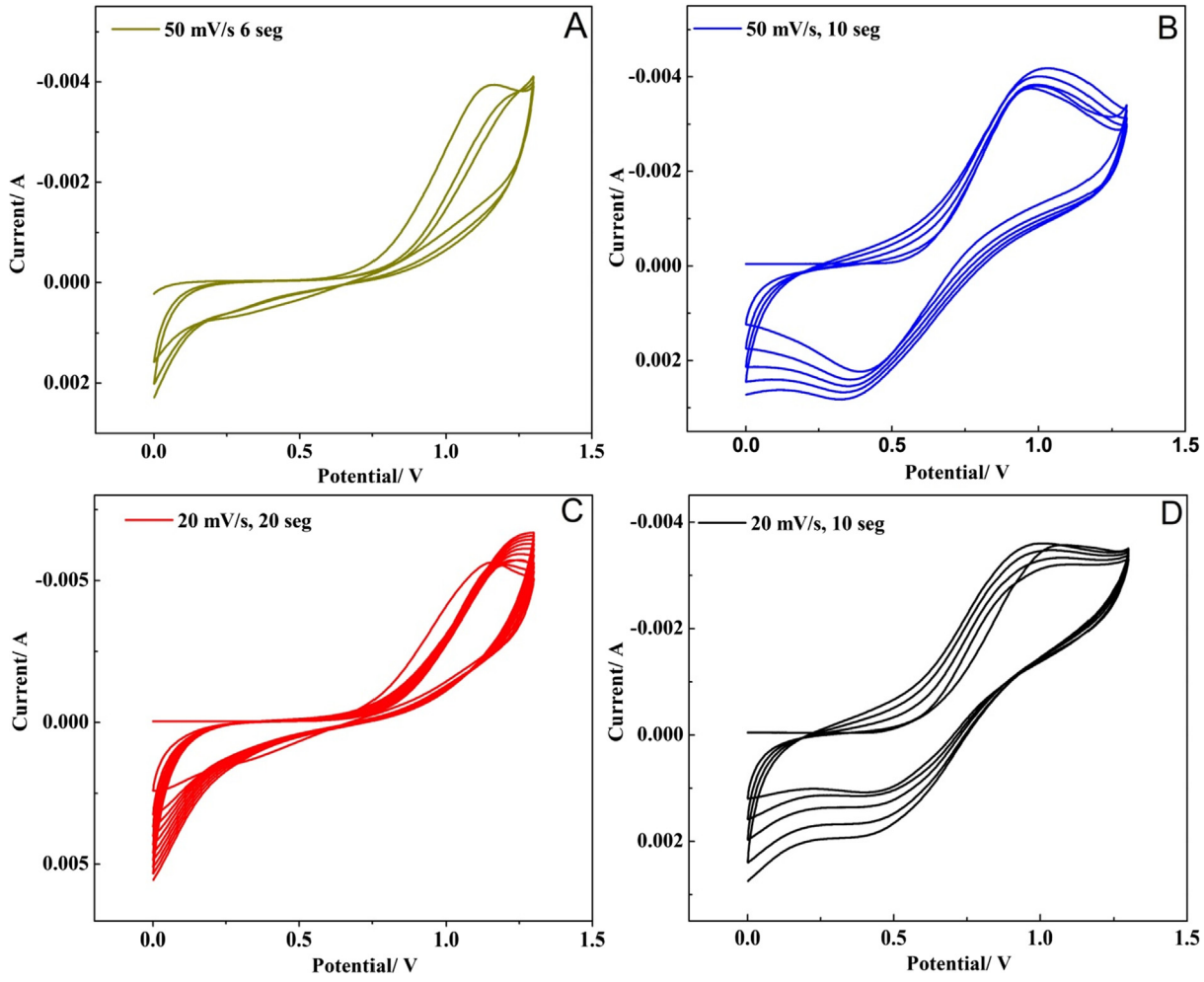

Fig. 1 Cyclic voltamogrammes of the preparation electrode (A) deposition at 50 mV/s, 6 segments (50/6), (B) deposition at 50 mV/s, 10 segments (50/10), (C) deposition at 20 mV/s, 20 segments (20/20), (D) deposition at 20 mV/s 10 segments (20/10) in 1.0 M Na_2SO4 solution. (Optimum is 'D').

tained the scan rates at 20 mV at 10 segments. The formation of Mn^+ ion and Ni^+ ion occurs, where the hydroxide (OH^-) ions are localized. The metal hydroxide nanostructure was formed between Mn^+/Ni^+ cations and OH^- ions. Finally bimetal oxide nanoflakes were obtained on the substrate during the annealing process (Rusi et al., 2014).

3.2. Morphological studies

The surface morphology of GO/MnO_2-NiO/SS electrodes was studied by field emission scanning electron microscopy. The SEM images for electrodes employed various cyclic voltammetric scan rates and cycles, were shown in Fig. S3. Based on the observed, well defined cyclic voltamogrammes (Fig. S4) and well organised nanostructure [Fig. 2 (A, B different magnifications] of the sample obtained at scan rate 20 mV/s for 10 segments and subsequent annealing at 400°C for 4 h, the sample is denoted as (20/10), it was selected as the suitable and optimum sample and used for further application. Fig. 2 clearly shows that the nanoflakes of bimetal oxide (MnO_2-NiO) nano structure formed over the steel substrate. Further, Fig. S3 (E) and Fig. S3 (F) present the SEM images of MnO_2-NiO nanoflakes incorporated with 10 μL and 50 μL of graphene oxide respectively. The graphene oxide layer was clearly observed on MnO_2-NiO nanoflakes. Based on the quality appearance of nanostructure the nano flakes formed by 30 μL of GO was selected as optimum sample, [Fig. 2(C)]. In addition Energy-dispersive X-ray spectroscopy (EDX) was also carried out for the electrodes; The EDX recorded at the portion, marked by pink colored square of Fig. 2(A), indicates the presence of Mn, Ni, and O elements and carbon, originated from graphene oxide in the sample, the corresponding EDX spectra shown in Fig. S5 It can be confirmed that graphene oxide and MnO_2-NiO nanoflakes were well formed on the steel substrate.

X-Ray diffraction studies were used to examine the crystalline nature and structural details of nano structure of bimetal oxide (Mn-Ni). The obtained XRD patterns of bimetal oxide (Mn-Ni) based nanoflakes are shown in Fig. 3. The XRD peaks observed were attributed to MnO_2-NiO nanoflakes and can be indexed to MnO_2 [JCPDS card no. 44-0141] and NiO [JCPDS card no. 78-0643]. The sharp and

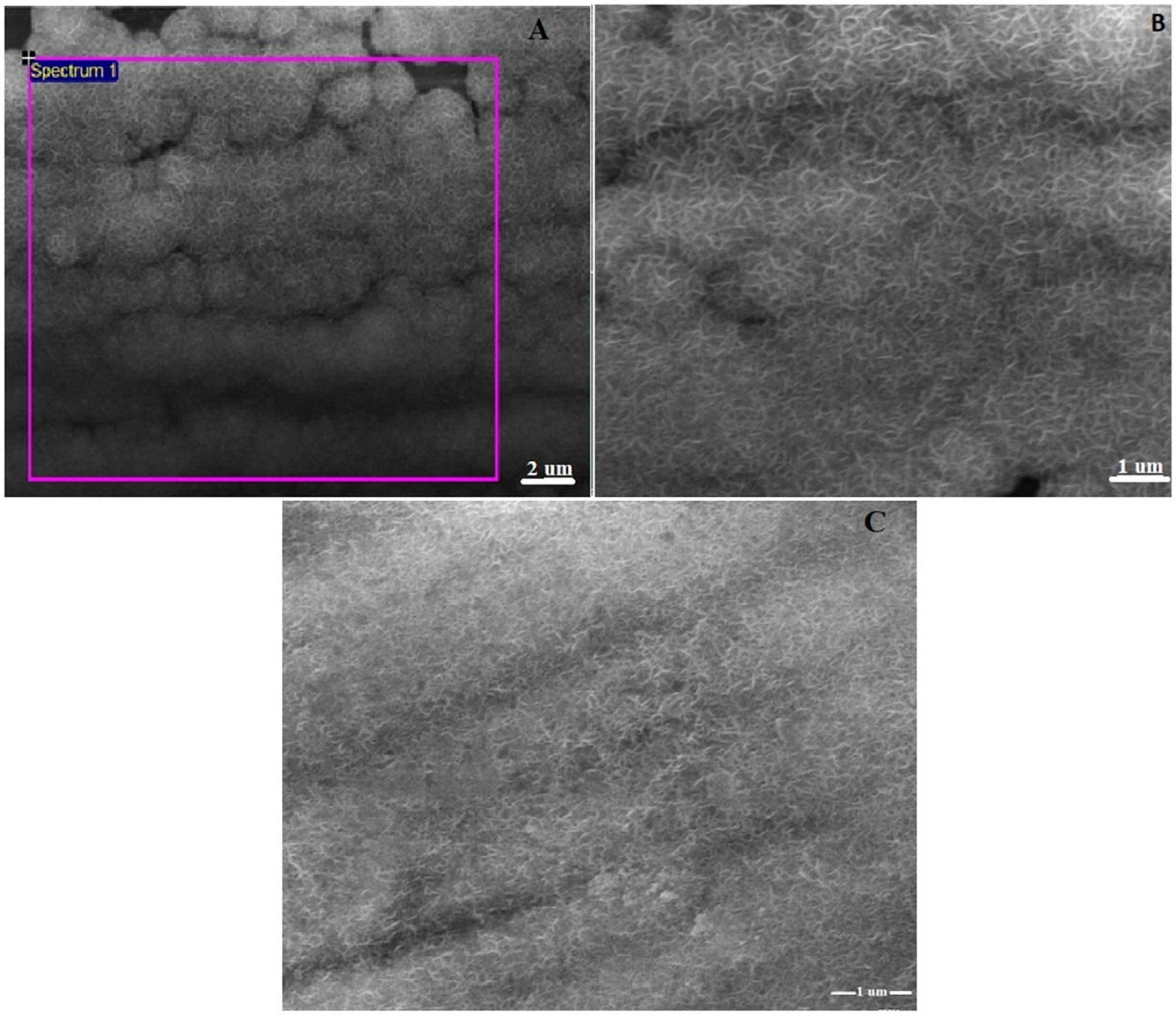

Fig. 2 SEM images of the electrode MnO_2-NiO flakes (A,B different magnifications) at 20/10, and graphene oxide decorated MnO2-NiO nanoflakes at 30 GO (C).

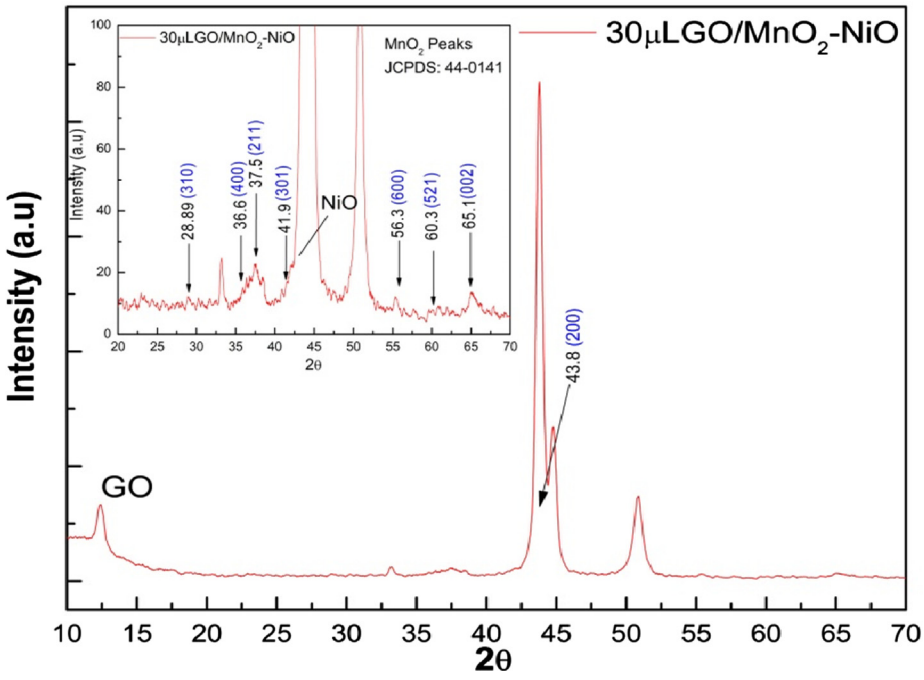

Fig. 3 XRD patterns of the as prepared electrode 30 μL GO/MnO_2-NiO (30GO) electrode, annealing at 200° C for 2 h and, (Inset enlarged view of XRD patterns).

intense diffraction peaks of MnO_2-NiO flakes confirm that the samples possess good crystalline nature. A broad hump observed at approximately $2\theta \sim 12°$ which can be ascribed to the amorphous phase of the nanostructure. The semi crystalline and amorphous phases have their origin in the employed cyclic sweeps, scan rate, deposition time, and annealing temperature. The peaks found at angles $2\theta \sim 28.89°$ and $2\theta \sim 37.5°$, $2\theta \sim 41.9°$, $2\theta \sim 56.3°$, and $2\theta \sim 65.1°$ which correspond to the (3 1 0), (2 1 1), (3 0 1), (6 0 0) and (0 0 2) respectively, are attributed to the MnO_2 and the peaks observed at around $2\theta \sim 43.8°$ that correspond (2 0 0) diffraction planes, is related to NiO (Hawang et al., 2013; Rusi et al., 2014) Some electrodes (prepared at high scan rates and more cycles) had shown low intensity XRD peaks, which explains that the MnO_2-NiO nanostructures possess poor crystallinity, this is in contrast with the nanoflakes having a superior specific area (Rusi et al., 2016). Furthermore a well-resolved XRD peak was found at around $2\theta \sim 12.0°$, which corresponds to the graphene oxide incorporated in to prepared electrode, the enlarged view of (GO/MnO_2-NiO) 30 GO XRD patterns are shown in Fig. 3. The present results were compared with existing reports and found that good agreement with those reported methods (Rusi et al., 2016; Lee et al., 2014; Rusi et al., 2014).

The TEM studies were carried out to investigate the microstructural details of the as prepared MnO_2-NiO nano structure based electrodes. The monitored TEM images are shown in Fig. 4, where Fig. 4 (a) depicts a cluster of 30 GO composite which clearly reveals rumple like structure [inset] which is attributed to the nanoflake morphology. The graphene oxide layers [marked using red coloured arrows in Fig. 4(a)], are found to be well combined with the MnO_2-NiO composite, indicating that the graphene oxide, well composited with the nanoflake MnO_2- NiO composite. The distinctive composite structure and homogeneous nano flake structure play a significant desired functional role for electrochemical application as an active material with a quick diffusion rate through the redox phase. The selected area electron diffraction (SAED) pattern of several thin sheets of the 30 GO (GO/MnO_2-NiO) [Fig. 4(b)] displays two sets of intense and bright spots forming clear rings correspond to the both MnO_2 and NiO nano composite structure, signifying the related crystallinity. The observed intense SAED ring patterns are indexed to (1 1 0), (1 0 1) and (2 1 1), planes of MnO_2 for d-spacing, ~0.311 nm, ~0.240 nm and ~0.162 nm respectively according to the JCPDF card No: 81–2261. Additional reflections from (1 1 1) and (2 0 0) planes correspond to the NiO for d-spacing ~0.241 nm and ~0.208 nm respectively are found to be in accordance with the JCPDF card No: 78-0643. These observations from SAED patterns are in good agreement with that of XRD studies. In addition, HRTEM image [Fig.(c)] depicts highly crystalline interconnected lattice portions and amorphous layer located at the edges of crystalline portions. The deeper insight in to the micro structure of the lattice is obtained by analysing the high-resolution TEM (HRTEM) lattice image [Fig.(d)]. The FFT images [insets of Fig. 4(d)] represent two distinguished lattice portions that correspond to the MnO_2 and NiO. The lattice fringes of MnO_2 crystalline structure were viewed along (1 1 1) and indexed for atomic planes($\bar{1}$ 10), (01 $\bar{1}$).and (10 $\bar{1}$).with lattice spacing ~ 0.311 nm, ~0.240 nm and ~0.240 nm respectively. The lattice planes correspond to NiO, ($\bar{1}$ 11), (1 1 1) and (2 0 0) were well resolved when viewed along the zone axis (0 $\bar{1}$ 1) which are belonging to the inter planar spacings of ~0.241 nm, ~0.241 nm and ~ 0.208 nm respectively (Rusi et al., 2016; Lee et al., 2014; Rusi et al., 2014). These observations ensure that the nano crystalline structures of MnO_2 and NiO co-exist in to a

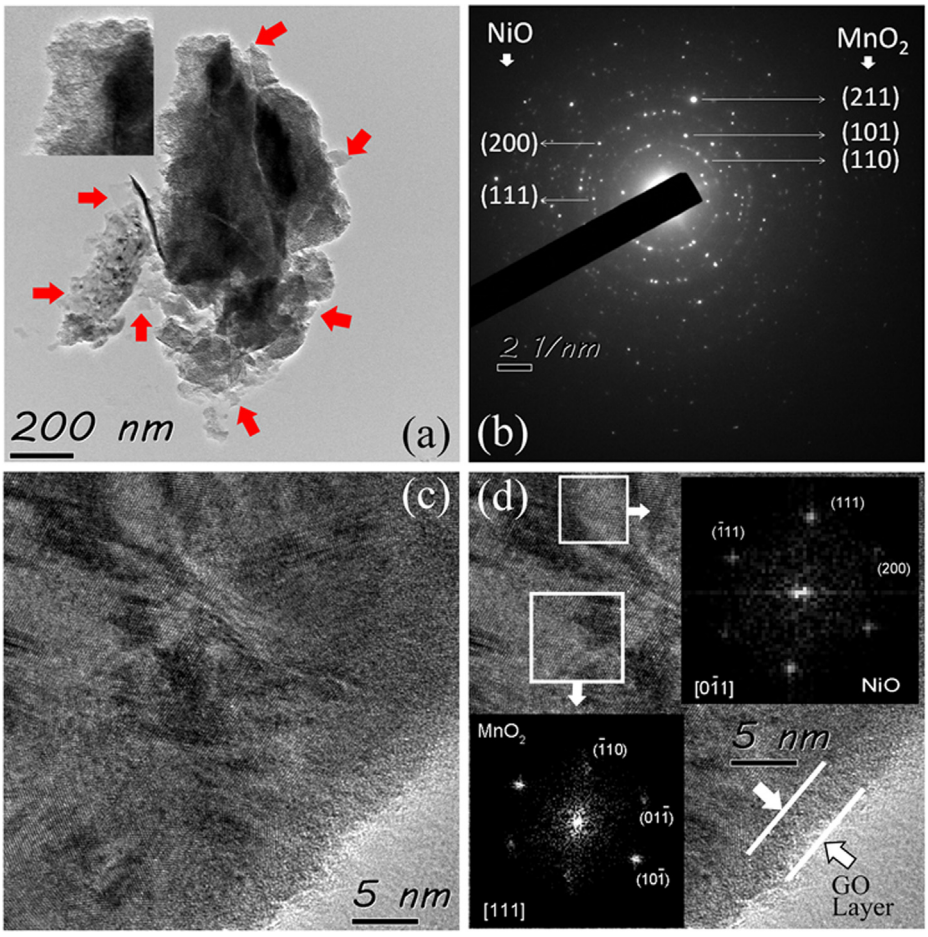

Fig. 4 TEM images of MnO_2-NiO nanoflakes with GO (a), SAED patterns of MnO_2-NiO nano flakes (b), HRTEM image of 30 GO (c), and HRTEM image of 30 GO with FFT MnO_2-NiO (d).

composite form. In addition, it is clearly found that the MnO_2-NiO composite is well combined with GO which is shown using two parallel lines at the edges of the composite nano structure. These observations are in consistent with that of FESEM, XRD and TEM studies.

Electrochemical impedance spectroscopy (EIS) was extensively used for studying the electron transfer between the electrolyte and the electrode surface employed. The impedance plot is usually characterized by a combination of semicircular arch of high frequency region and a straight line portion of low frequency range. The earlier corresponds to the charge (electron) transfer resistance (Rct) and can be obtained from the diameter of the arch, while the later, is associated to the electron diffusion process. The charge transfer resistance (Rct) influences the conductivity of the electrode and thus electron transfer in to the electrochemical reaction process. Fig. 5 depicts the Nyquist plots monitored for different electrodes under the applied frequency ranging from 0.01 Hz to 100 kHz. It can be clearly seen from the figure that the Nyquist plot of MnO_2-NiO electrode exhibit the largest semicircle with some portion as straight line. The diameter of the semi-circle is measured on the X-axis as Z″Ω, which indicates that the electrode has very high charge transfer resistance and a poor electron diffusion, during reaction process. This indicates poorer electrochemical activity and lower conductivity of MnO_2-

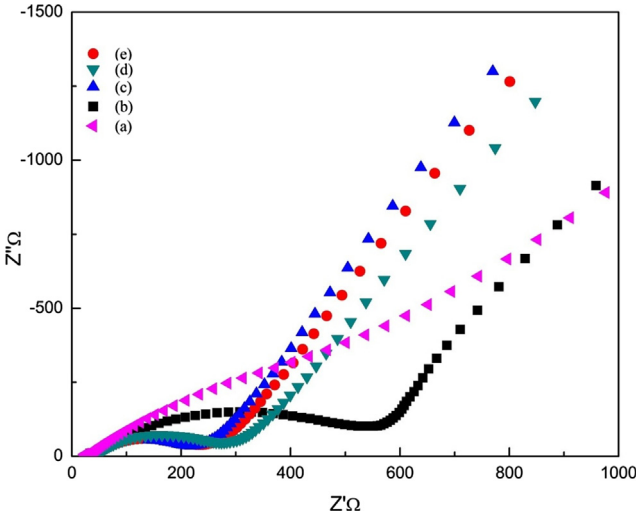

Fig. 5 Nyquist plots from EIS for all referred electrodes [(a) MnO_2-NiO/SS, (b) 50 μL GO-MnO_2-NiO/SS without annealing, (c) 30 μL GO-MnO_2-NiO/SS, (d) 20 μL GO-MnO_2-NiO/SS (e) 10 μL GO-MnO_2-NiO/SS] in 0.1 M KOH solution applied frequency between 100 kHz and 0.01 Hz.

NiO electrode. The measured values of Rct for MnO_2-NiO flakes treated with different amounts of graphene oxide are ranging from 200 Ω to 600 Ω as shown in the Fig. 5(a,b). The Rct of the MnO_2-NiO electrodes gradually decreases with the amount of graphene oxide decreased from 50 µL to 10 µL (followed the order c < e < d < b < a). It is found that the 30µLGO/MnO_2-NiO (30 GO) exhibits the lowest charge transfer resistance, signifying that the electrolyte sample possess a good electron diffusion mechanism, which is possibly due to the interconnected structure of obtained nano flakes and GO, and is in good agreement with the observed SEM and TEM images. The above results confirm that the 30 GO electrode has superior electrochemical activity than the remaining electrodes, the order (a < b < d < e < c) is indicating that the electrode exhibit a synergistic effect of the constituent nanomaterials.

3.3. Electrochemical performance of the electrode towards oxygen evolution reaction (OER)

Linear sweep voltammetry was used in order to demonstrate the elastrochemical performance of the electrodes, the OER behavior of MnO_2-NiO flakes and GO/MnO_2-NiO are examined through in 0.1 M KOH at a sweep rate of 10 mV/s, and

$$Mn/Ni2^{+} + 3OH^{-} \leftrightarrow Mn/NiOOH + H_2O + e^{-}$$

$$Mn/Ni(OOH) + OH^{-} \leftrightarrow Mn/NiOOH) + e^{-}$$

$$Mn/NiO(OH)_2 + OH^{-} \leftrightarrow Mn/Ni(OO_2) + 2H_2O + 2e^{-}$$

$$Mn/Ni(OO_2) + OH^{-} \rightarrow Mn/NiOOH + O_2 + e^{-}$$

$$\text{Overall OER: } 4OH^{-} \leftrightarrow O_2 + 2H_2O + 4e^{-}$$

Scheme 3

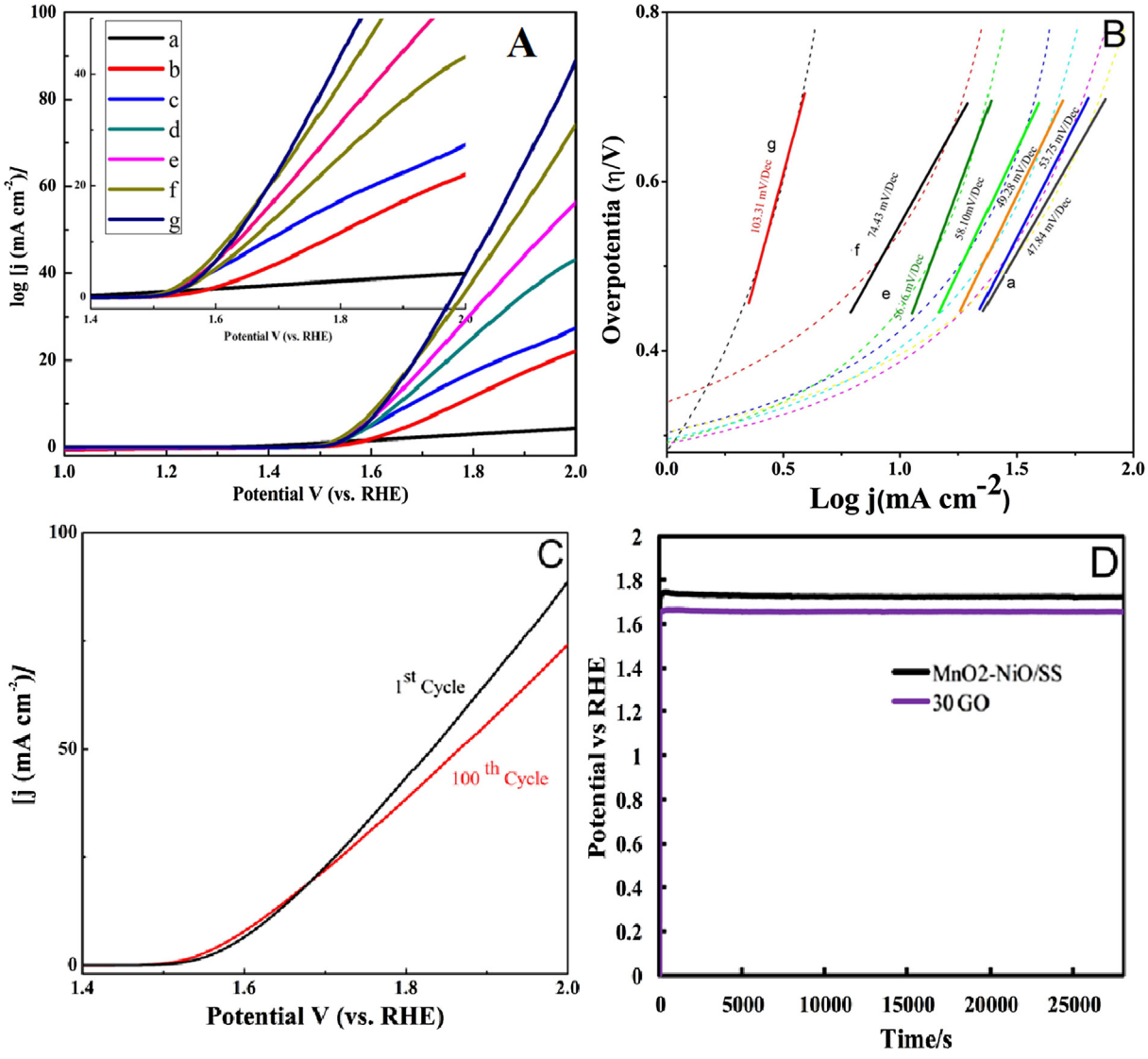

Fig. 6 Linear sweep voltammetric curves of various electrodes [A] (a) SS, (b) MnO_2-NiO, (c) MnO_2-NiO with annealing, (d) 10 GO, (e) 20 GO, (f) 50 GO, (g) 30 GO (inset enlarged view of LSV curves, [B] Tafel plates for various electrodes [(a) SS, (b) MnO_2-NiO, (c) MnO_2-NiO with annealing, (d) 10 GO, (e) 20 GO, (f) 50 GO, (g) 30 GO], [C] Durability of the 30 GO electrode for 100 cycles. [D] Durability of the various electrodes MnO_2-NiO and 30 GO using chronopotentiometry at j: 10 mV/cm^2.

Table 1 Comparison of OER activity on Mn and Ni related electrodes/catalysts.

Electrode/Catalyst	Overpotential (V)	Tafel slope (mV/Dec)	Ref
30 μL GO/MnO_2-NiO	0.379	47.84	Present
Mn-Ru Oxides	0.259 ± 0.016	48 ± 2	Browne et al. (2016)
MnO_X	0.60	120 to 70	Michael et al. (2015)
NiO_x, MnO_x, and FeO_x	0.24–0.27	32–36	Morales Guio et al. (2016)
NiO/Ni nanosheets	0.26	51	Yushuai et al., 2017
CoMn LDH	0.35	43	Song and Hu (2014)
Ni–Fe–OH	0.316	53	Wu et al. (2019)
MnO_X bi layers	0.45	–	Kang et al. (2017)
Gr-MnO_2	0.20	–	Chen et al. (2014)
H–TiO_2/MnOx NWs	0.524	–	Li et al. (2015)

the results are shown in Fig. 6. It is found that the potentials vs RHE of oxygen evolution reaction are 1.768 V, 1.689 V, 1.658 V, 1.64 V, 1.62 V and 1.609 V and corresponding to overpotential are 0.539 V, 0.458 V, 0.43 V, 0.418 V, 0.398 and 0.379 V for electrodes based on the MnO_2-NiO, MnO_2-NiO annealing, 10 GO, 20 GO, 50 GO and 30 GO, respectively.

The lowest onset potential is exhibited by 30 GO based electrode indicating that it is highly active anode materials towards OER application. Hence a fast OER activity can easily be achieved by the 30 GO electrode. The possible reaction mechanism was shown in Scheme 3. Further the current density values measured from the polarization curves obtained under the applied potentials ranging from 0.6 V to 0.8 V for the prepared electrodes based on different amounts of graphene oxide at 10 mA cm^{-2} current density. It can be seen from the Fig. 6A, that the OER activity was increased up to 30 μL of graphene oxide and then decreased with the concentration of GO. The substrate SS (a), MnO_2-NiO (b), annealed MnO_2-NiO (c) showed poor activity of the OER and the MnO_2-NiO flakes treated with graphene oxide (d-g), exhibited a higher activity suggests that the electrocatalyst is a potential catalyst for achieving significant activity. The enhanced OER activity and current density can be related to the flake like nanostructure of MnO_2-NiO-GO, increased electrode surface area and also the synergistic effect between the metal oxides. The photography was taken while water oxidation process shown in Fig. S6, we can see that the bubbles were clearly formed on the working electrode. It's evident that the as prepared electrode exhibits good OER catalytic activity.

The Tafel slope of the as prepared electrodes serves a key indicator to assess the performance of oxygen evolution. The Tafel slopes measured from the linear portion of the curves [Fig. 6B] of the range potentials vs RHE around from 1.6 V to 1.8 V for various electrodes (different cyclic sweeps, scan rates and graphene oxide) are given in Table 1 which indicates good OER activity. From the Table 1 it can be observed that 30 μL GO/MnO_2-NiO (30 GO) electrode displays the lower Tafel slope of 47.84 mV dec^{-1}, which is similar to that of bench mark electro catalysts (Browne et al.,2016; Chen et al., 2014; Li et al., 2015). The obtained results suggest that the electrode 30 μL GO/MnO_2-NiO exhibits a good catalytic performance of oxygen evolution. The electrodes especially graphene oxide deposited MnO_2-NiO flakes (10–50 μL GO/MnO_2-NiO) exhibit Tafel slopes lying between 58 and 49 mV/dec. The lower Tafel slopes reveal that the graphene oxide layer was deposited well with metal oxides nanoflakes and played significant role in OER behaviour.

Furthermore the stability of the electrodes was examined by linear sweep voltammetry and chronoamperometry. As shown in Fig. 6C, the comparative LSV curves up to 100 cycles have no big change in the current density and OER activity. Furthermore according to the stability study using chronoamperometry both the electrodes MnO_2-NiO and 30 μL GO/MnO_2-NiO (30 GO) exhibit good stability up to 28,800 sec, no dispersion from the straight behavior or fall down in the curve is found, as seen from the Fig. 6D. The results clearly prove that when the graphene oxide decorated, the OER potential was decreased it shows that as prepared electrodes exhibit good OER stability.

4. Conclusions

The bimetal oxides (MnO_2-NiO) and graphene oxide mixed composite electrodes GO/MnO_2-NiO were synthesized and their anodic water oxidation activities in an aqueous alkaline solution were studied. The main parameters such as mixture of (MnO_2-NiO-GO) oxide composition, deposition cycles, scan rate, annealing temperature, and annealing time influenced the development of the nanostructure and OER activity. The combination of these mixed oxides shows superior activity for oxygen evolution at a low overpotential. The electro catalyst contained GO and employed Mn-Ni precursor solutions deposited at various scan rates (10–50 mV/s for 6–20 cycles, show good OER activity regarding overpotential and Tafel slopes, present results are comparable to that of previous reports and hence the present novel composite electrode material is feasible for electrocatalytic reaction. The present method significantly contributes to the development of ongoing research by employing the combination of transition metal oxides for OER catalysts. The enhanced OER activity was attributed to the changing electronic state of the metal oxides and the crystallinity of the nanostructure was influenced by the annealing temperature and time. The present method of synthesis of new combination of the materials is less expensive, simple and feasible for implementation in comparison with that of the expensive pure Ru and Ir materials. Further, when compared with the platinum group oxides combined with the first row transition metal oxides, the present method facilitates high OER activity, and hence the composite is a promising alternative electrocatalyst for OER application.

Acknowledgment

This work was supported by the National Natural Science Foundation of China under the Grant Nos. 51661033, 51361028, 51161025 and 31660538.

Declaration of Competing Interest

There are no conflicts to declare.

Appendix A. Supplementary material

Supplementary data to this article can be found online at https://doi.org/10.1016/j.arabjc.2019.10.003.

References

Antolini, E., 2014. Iridium As catalyst and cocatalyst for oxygen evolution/reduction in acidic polymer electrolyte membrane electrolyzers and fuel cells. ACS Catal. 4, 1426–1440.

Arpita, J., Scheer, E., Polarz, S., 2017. Synthesis of graphene–transition metal oxide hybrid nanoparticles and their application in various fields. Beilstein J. Nanotechnol. 8, 688–714.

Batchellor, A.S.W.S., 2015. Boettcher, Pulse-electrodeposited Ni-Fe (oxy) hydroxide oxygen evolution electrocatalysts with high geometric and intrinsic activities at large mass loadings. ACS Catal. 5, 6680–6689.

Browne, M.P., Nolan, H., Duesberg, G.S., Colavita, P.E., Lyons, M. E., 2016. Low-overpotential high-activity mixed manganese and ruthenium oxide electrocatalysts for oxygen evolution reaction in alkaline media. ACS Catal. 6, 2408–2415.

Chen, S., Duan, J.J., Han, W., Qiao, S.Z., 2014. A graphene–MnO_2 framework as a new generation of three-dimensional oxygen evolution promoter. Chem. Commun. 50, 207–209.

Chi, J.Q., Shang, X., Gao, W.K., Dong, B., Yan, K.L., Li, X., et al, 2017. Binary metal $Fe0.5Co_{0.5}Se_2$ spheres supported on carbon fiber cloth for efficient oxygen evolution reaction. Int. J. Hydrogen Energy 42, 15189e95.

Chu, S., Majumdar, A., 2012. Opportunities and challenges for a sustainable energy future. Nature 488, 294.

Danilovic, N., Subbaraman, R., Chang, K.C., Chang, S.H., Kang, Y., Snyder, J., Paulikas, A.P., Strmcnik, D., Kim, Y.T., Myers, D., Stamenkovic, V.R., Markovic, N.M., 2014. Using surface segregation to design stable Ru-Ir oxides for the oxygen evolution reaction in acidic environments. Angew. Chem. Int. Ed. 53, 14016–14021.

Darabdhara, G., Amin, M.A., Mersal, G.A.M., Ahmed, E.M., Das, M.R., Zakaria, M.B., Malgras, V., Alshehri, S.M., Yamauchi, Y., Szuneritsj, S., Boukherroub, R., 2015. Reduced graphene oxide nanosheets decorated with Au, Pd and Au–Pd bimetallic nanoparticles as highly efficient catalysts for electrochemical hydrogen generation. J. Mater. Chem. A 3, 20254–20266.

Guio Morales, C.G., Stern, L.A., Hu, X., 2014. Nanostructured hydrotreating catalysts for electrochemical hydrogen evolution. Chem. Soc. Rev. 43, 6555–6569.

Huang, C., Zou, Y., Ye, Y.-Q., Ouyang, T., Xiao, K., Liu, Z.-Q., 2019. Unveiling the active sites of Ni–Fe phosphide/metaphosphate for efficient oxygen evolution under alkaline conditions. Cite this: Chem. Commun 55, 7687.

Hutchings, G.S., Zhang, Y., Li, J., Yonemoto, B.T., Zhou, X.G., Zhu, K.K., Jiao, F., 2015. In situ formation of cobalt oxide nanocubanes as efficient oxygen evolution catalysts. J. Am. Chem. Soc 137, 4223–4229.

Hwang. S. Gi, Hong, J. Eui, Kim, GOK, Jeong, H. Mo, Ryuz, K. Sun, 2013. The electrochemical society, graphene anchored with NiO-MnO2 nanocomposites for use as an electrode material in supercapacitors. ECS Solid State Lett. 2 (1) (2013) M8–M11.

Kang, Q., Vernisse, L., Richard, R.C., Akila, T.C., Samantha, S.L., McKendry, I.G., Klein, M.L., Borguet, E., Zdilla, M.J., Daniel, S. R., 2017. Effect of interlayer spacing on the activity of layered manganese oxide bilayer catalysts for the oxygen evolution reaction. J. Am. Chem. Soc. 139, 1863–1870.

Lee, H.Min., Lee, K., Koo Kim, C., 2014. Electrodeposition of manganese-nickel oxide films on a graphite sheet for electrochemical capacitor applications. Materials 7, 265–274. https://doi.org/10.3390/ma7010265.

Lee, Y., Suntivich, J., May, K.J., Perry, E.E., Shao-Horn, Y., 2012. Synthesis and activities of rutile IrO_2 and RuO_2 nanoparticles for oxygen evolution in acid and alkaline solutions. J. Phys. Chem. Lett. 3, 399–404.

Li, R., Liu, Y., Li, H., Zhang, M., Yiran, L., Zhang, L., Xiao, J., Boehm, F., Yan, K., 2019. One-step synthesis of NiMn-layered double hydroxide nanosheets efficient for water oxidation. Small Methods 3, 1800344.

Li, N., Yan Xia, W., Wang, J., Li Liu, Z., Yu Li, Q., Zhou Chen, S., Wei Xu, C., Hong Lu, X., 2015. Manganese oxides supported on hydrogenated TiO_2 nanowire array catalysts for the electrochemical oxygen evolution reaction in water electrolysis. J. Mater. Chem. A 3, 21308.

Lu, Y.X., Zhao, C., 2015. Electrodeposition of hierarchically structured threedimensional nickel-iron electrodes for efficient oxygen evolution at high current densities. Nat. Commun. 6, 6616.

McKone, J.R., Sadtler, B.F., Werlang, C.A., Lewis, N.S., Gray, H.B., 2013. Ni–Mo nanopowders for efficient electrochemical hydrogen evolution. ACS Catal. 3 (2), 166–169.

Menezes, P.W., Indra, A., Sahraie, N.R., Bergmann, A., Strasser, P., Driess, M., 2015. Cobalt–manganese-based spinels as multifunctional materials that unify catalytic water oxidation and oxygen reduction reactions. ChemSusChem 8, 164–171.

Michael, H., Chenyang, S., Billinge, S.J.L., Nocera, D.G., 2015. Nature of activated manganese oxide for oxygen evolution. J. Am. Chem. Soc 137 (47), 14887–14904.

Morales Guio, C.G., Liardet, L., Hu, X.L., 2016. Oxidatively electrodeposited thin-film transition metal (oxy)hydroxides as oxygen evolution catalysts. J. Am. Chem. Soc. 138, 8946–8957.

Oh, H.S., Black, R., Pomerantseva, E., Lee, J.H., Nazar, L.F., 2012. Synthesis of a metallic mesoporous pyrochlore as a catalyst for lithium-O2 batteries. Nat. Chem. 4, 1004–1010.

Oh, H.S., Nong, H.N., Reier, T., Gliech, M., Strasser, P., 2015. Oxide-supported Ir nanodendrites with high activity and durability for the oxygen evolution reaction in acid PEM water electrolyzers. Chem. Sci. 6, 3321–3328.

Park, S., Shao, Y., Liu, J., Wang, Y., 2012. Oxygen electrocatalysts for water electrolyzers and reversible fuel cells: status and perspective. Energy Environ. Sci. 5, 9331–9344.

Pei, Y., Yuancai, G., Chu, H., Smith, W., Dong, P., Ajayan, P.M., Ye, M., Shen, J., 2019. Controlled synthesis of 3D porous structured cobalt-iron based nanosheets by electrodeposition as asymmetric electrodes for ultra-efficient water splitting. Appl. Catal. B 244, 583–593.

Prasad. M. Siva, Hongwei, R. Chen, Ni, H., Kumar, K. Kiran, 2020. Directly grown of 3D-nickel oxide nano flowers on TiO2 nanowire arrays by hydrothermal route for electrochemical determination of naringenin flavonoid in vegetable samples, Arab. J. Chem. 13, 1520–1531. doi.org/10.1016/j.arabjc.2017.12.004..

Qiao, C., Zhang, Y., Zhu, Y.Q., Cao, C.B., Bao, X.H., Xu, J.Q., 2015. One-step synthesis of zinc–cobalt layered double hydroxide (Zn–Co-LDH) nanosheets for high-efficiency oxygen evolution reaction. J. Mater. Chem. A 3, 6878–6883.

Reier, T., Oezaslan, M., Strasser, P., 2012. Electrocatalytic oxygen evolution reaction (OER) on Ru Ir, and Pt catalysts: a comparative study of nanoparticles and bulk materials. ACS Catal. 2, 1765–1772.

Rong, F., Zhao, J., Su, P.P., Yao, Y., Li, M.R., Yang, Q.H., Li, C., 2015. Zinc–cobalt oxides as efficient water oxidation catalysts: the promotion effect of ZnO. J. Mater. Chem. A 3, 4010–4017.

Rusi, S.R., Majid, 2014. High performance super-capacitive behaviour of deposited manganese oxide/nickel oxide binary electrode system. Electrochim Acta. 138, 1–8.

Rusi, S.R., Majid, 2016. Effects of electrodeposition mode and deposition cycle on the electrochemical performance of MnO_2-NiO composite electrodes for high-energy-density supercapacitors. PLOS ONE. https://doi.org/10.1371/journal.pone.0154566.

Senthil, R.A., Junqingn, P., Yang, X., Sun, Y., 2018. Nickel foam-supported NiFe layered double hydroxides nanoflakes array as a greatly enhanced electrocatalyst for oxygen evolution reaction. Int. J. Hydrogen Energy 43, 21824–21834.

Singh, S.K., Dhavale, V.M., Kurungot, S., 2015. Low surface energy plane exposed Co_3O_4 nanocubes supported on nitrogen-doped graphene as an electrocatalyst for efficient water oxidation. ACS Appl. Mater. Interfaces 7, 442–451.

Song, F., Hu, X.L., 2014. Ultrathin cobalt-manganese layered double hydroxide is an efficient oxygen evolution catalyst. J. Am. Chem. Soc 136, 16481–16484.

Suntivich, J., May, K.J., Gasteiger, H.A., Goodenough, J.B., Shao Horn, Y., 2011. A perovskite oxide optimized for oxygen evolution catalysis from molecular orbital principles. Science 334, 1383–1385.

Takashima, T., Hashimoto, K., Nakamura, R., 2012. Inhibition of charge disproportionation of MnO_2 electrocatalysts for efficient water oxidation under neutral conditions. J. Am. Chem. Soc 134, 18153–18156.

Tan, C.F., Azmansah, S.A.B., Zhu, H., Xu, Q.-H., Ho, G.W., 2017. spontaneous electroless galvanic cell deposition of 3D hierarchical and Interlaced S-M–S heterostructures. Adv. Mater. 29, 1604417.

Tran. M. Van, A. The Ha, Le, P. My Loan, Nanoflake manganese oxide and nickel-manganese oxide synthesized by electrodeposition for electrochemical capacitor, J. Nanomater. 2015, Article ID 609273.

Wang, T.H., 2015. Bifunctional non-noble metal oxide nanoparticle electrocatalysts through lithium-induced conversion for overall water splitting. Nat. Commun. 6, 7261.

Wang, X.-T., Ouyang, T., Wang, L., Zhong, J.-H., Ma, T., Liu, Z.-Q., 2019. Redox-Inert $Fe3+$ Ions in octahedral sites of Co-Fe spinel oxides with enhanced oxygen catalytic activity for rechargeable zinc-air batteries. Angew. Chem. Int. Ed. 58, 13291–13296.

Wang, Y., Yan, D., Hankari, S.E., Zou, Y., Wang, S., 2018. Recent progress on layered double hydroxides and their derivatives for electrocatalytic water splitting. Adv. Sci. 5, 1800064.

Wu, L.K., Xia, J., Hou, G.-Y., Cao, H.-Z., Tang, Y.-P., Zheng, G.-Q., 2016. Potentiodynamical deposition of nanostructured MnO_2 film at the assist of electrodeposited SiO_2 as template. Electrochim. Acta 191, 375–384.

Wu, L.K., Zhu, Y.X., Liu, M., Hou, G.Y., Ping Tang, Y., Zhen Cao, H., Bin Zhang, H., Qu Zheng, G., 2019. Ultrafast fabrication of amorphous bimetallic, hydroxide layer on nickel nano cones array for oxygen evolution electrocatalyst. Int. J. Hydrogen Energy 44, 5899–5911.

Xie, J., Zhang, J., Li, S., Grote, F., Zhang, X., Zhang, H., Wang, R., Lei, Y., Pan, B., Xie, Y., 2013. Controllable disorder engineering in oxygen-incorporated MoS2 ultrathin nanosheets for efficient hydrogen evolution. J. Am. Chem. Soc. 135, 17881–17888.

Yan, D., Dong, C.L., Huang, Y.C., Zou, Y., Xie, C., Wang, Y., 2018. Engineering the coordination geometry of metal-organic complex electrocatalysts for highly enhanced oxygen evolution reaction. J. Mater. Chem. A 6, 805e10.

Yan, Q., Yan, P., Wei, T., Wang, G., Cheng, K., Ye, K., Zhu, K., Yan, J., Cao, D., Li, Y., 2019. A highly efficient and durable water splitting system: platinum sub-nanocluster functionalized nickel–iron layered double hydroxide as the cathode and hierarchical nickel–iron selenide as the anode. J. Mater. Chem. A 7, 2831.

Yang, Y., Shi, M., Li, Y.-S., Fu, Z.-W., 2012. MnO_2-graphene composite air electrode for rechargeable Li-air batteries. J. Electrochem. Soc. 159, A1917–A1921.

Yang, M.Q., Xu, Y.J., Lu, W., Zeng, K., Zhu, H., Xu, Q.-H., Ho, G. W., 2017. Self-surface charge exfoliation and electrostatically coordinated 2D hetero-layered hybrids. Nat. Commun. 8, 14224.

Ye, Z., Li, T., Ma, G., Dong, Y., Zhou, X., 2017. Metal-ion (Fe, V Co, and Ni)-doped MnO2 ultrathin nanosheets supported on carbon fiber paper for the oxygen evolution reaction. Adv. Funct. Mater., 1704083

Yushuai, X., Huang, K., Gang, O., Tang, H., Wei, H., Zhang, Q., Gong, J., Fang, M., Wu, H., 2017. A facile fabrication method for ultrathin NiO/Ni nanosheets as a high-performance electrocatalyst for the oxygen evolution reaction. RSC Adv 7, 18539.

Zhang, J., Wang, T., Pohl, D., Rellinghaus, B., Dong, R., Liu, S., Zhuang, X., Feng, X., 2016b. Interface engineering of MoS2 / Ni3S2 heterostructures for highly enhanced electrochemical overall-water-splitting activity. Angew. Chem. Int. Ed 55, 6702–6707.

Zhang, J., Wang, T., Liu, P., Liu, S., Dong, R., Zhuang, X., Chen, M., Feng, X., 2016c. Engineering water dissociation sites in MoS_2 nanosheets for accelerated electrocatalytic hydrogen production. Energy Environ. Sci. 9, 2789.

Zhang, B., Xiao, C., Xie, S., Liang, J., Chen, X., Tang, Y., 2016a. Iron-nickel nitride nanostructures in situ grown on surface-redox-etching nickel foam: efficient and ultrasustainable electrocatalysts for overall water splitting. Chem. Mater 28 (19), 6934–6941.

Zhenhua. Y., Hongming, S., Chen, X., Huanhuan, L., Zhao, Y., Haixia, L., Wei, X., Cheng, F., Chen, J., 2018. Anion insertion enhanced electrodeposition of robust metal hydroxide/oxide electrodes for oxygen evolution Nat. Commun. | (2018) 9:2373. DOI: 10.1038/s41467-018-04788-3.

Zhuang, Z.B., Sheng, W.C., Yan, Y.S., 2015. Precious-metal-free Co-Fe-O/rGO synergetic electrocatalysts for oxygen evolution reaction by a facile hydrothermal route. ChemSusChem 8, 659–664.

Zou, X., Zhang, Y., 2015. Noble metal-free hydrogen evolution catalysts for water splitting. Chem. Soc. Rev. 44, 5148–5180.